Haptic Contour Following and Feature Detection with a Contact Location Display

Jaeyoung Park[1], William R. Provancher[2], David E. Johnson[3] and Hong Z. Tan[1]

[1]Haptic Interface Research Laboratory, Purdue University, West Lafayette, IN, USA
[2]Haptics and Embedded Mechatronics Laboratory, University of Utah, Salt Lake City, UT, USA
[3]Geometric Design and Computation Laboratory, University of Utah, Salt Lake City, UT, USA

ABSTRACT

We investigate the role of contact location information on the perception of local features during contour following in a virtual environment. An absolute identification experiment is conducted under force-alone and force-plus-contact-location conditions to investigate the effect of the contact location information. The results show that the participants identify the local features significantly better in terms of higher information transfer for the force-plus-contact-location condition, while no significant difference was found for measures of the efficacy of contour following between the two conditions. Further data analyses indicate that the improved identification of local features with contact location information is due to the improved identification of small surface features.

KEYWORDS: contact location display, contour following, haptic feature detection

INDEX TERMS: H.5.2 [INFORMATION INTERFACES AND PRESENTATION]: User Interfaces (D.2.2,H.1.2,I.3.6)-Haptic I/O

1 INTRODUCTION

Until recently, if a user wanted to feel a virtual object via touch, it was through a force-feedback device in most cases. Most force displays are designed to render forces through single-point interactions between a tool tip and a virtual object's surface. One way to provide a user with increased haptic information is to increase the number of contact points by using multiple force feedback devices. Frisoli et al. showed, however, that increasing the number of force feedback contact points from one to three did not significantly improve virtual object recognition performance [1]. Jansson and Monaci also showed that without distributed information at contact areas, increasing the number of contact points alone did not lead to a significant benefit in identifying real objects. Instead, recognition of objects was significantly improved when spatially distributed information was available at each contact area on bare fingers [2]. The findings from the previous studies suggest that for improved haptic perception and exploration of virtual objects, it is desirable to provide not only point-contact force feedback but also cutaneous contact information. Several fingertip displays have been designed so far (e.g., [3-8]), including the contact location display (CLD) that is used in the present study [9].

Contact location information conveyed via fingertip displays contributes to haptic object exploration and perception in tasks such as contour following. Lederman and Klatzky show that during haptic exploration of an object, hand movements vary by the type of knowledge that one is trying to acquire about the object. A contour following exploratory procedure is typically used when the precise shape details of the object are desired [10]. Kuchenbecker et al. showed that cutaneous fingertip contact information improved the accuracy and reduced the time in a contour following task [11]. Contact information is therefore expected to play an important role in haptic shape exploration.

Contact information at the fingertip is especially important for the perception of small or detailed features on the surfaces of virtual objects. It has been shown that haptic object recognition requires information from both cutaneous and proprioceptive inputs, and that both SA1 and FA1 afferents provide information about the local geometrical form and texture at the location of contact [12, 13]. Considering the high density of the corresponding mechanoreceptors at the fingertip, the importance of cutaneous sensation at the fingertips cannot be overemphasized for haptic perception of object surface details [14].

In the present study, the contact location display (CLD) is used to provide a user with cutaneous cues on the fingertip. The overall haptic system used in the present study is a combination of the CLD and a commercially available force feedback device. Our haptic system can provide a user with both force and contact location information during haptic interactions with virtual surfaces. So far, the contributions of contact location information in virtual object manipulation and perception have been investigated in several studies by using the CLD haptic system.

The first CLD study measured human curvature discrimination thresholds using physical and virtual curvature models. The results show that the discrimination thresholds are similar for real and virtual curvatures [15]. A subsequent study evaluated the role of CLD on contour following. The results indicate decreased task time and fewer losses of surface contact with the aid of CLD than with force feedback alone [11]. The CLD was also used in the evaluation of a haptic rendering algorithm for rendering smooth surfaces when contact location information is available along with force feedback information [16].

In more recent CLD studies, the relative contributions of contact location and force information are investigated for the haptic perception of virtual edges. An edge sharpness discrimination experiment was conducted under two conditions: force feedback alone and force plus contact location information. While the discrimination thresholds under both conditions increase as the reference radius of virtual edge increases, no statistically significant difference is found between the two experiment conditions. The effect of the CLD's contact roller size for the edge sharpness discrimination task was evaluated in a subsequent study. The results indicate that the radius of the roller does not significantly affect the users' ability to discriminate edge sharpness, indicating that the users can overcome the effect of the roller's curvature by focusing on the roller's movement [17].

park183@purdue.edu, wil@mech.utah.edu, dejohnso@cs.utah.edu, hongtan@purdue.edu

While the advantage of the CLD in contour following was identified in a previous study, it was not studied whether and how improved contour following benefits haptic perception of surface shape features [11]. The present study investigates the contribution of the CLD to the detection of virtual surface features in the context of a contour following task. Our objectives are to assess the role of the contact location information in i) local feature identification, and ii) participants' ability to follow contours. For the first objective, we hypothesize that the addition of contact location cues to contact force information will improve the identification of small surface features, as small bumps are what cutaneous sensing is good for while larger bumps likely involve kinesthetic sensing. For the second objective, we hypothesize that contact location information will make contour following easier, which in turn will lead to better identification of surface features. We further hypothesize that the benefit of CLD would decrease as contour following slows down. In a real-life scenario of contour following and feature detection (e.g., exploration by a fingertip inserted into a surgical incision), it is always desirable to perform the task as efficiently as possible. Therefore, it was required that the participants in the present study perform the experimental task as quickly as possible.

In the remainder of the paper, we present methods (Sec. 2), results (Sec. 3) and discussion (Sec. 4).

2 METHODS

2.1 The Contact Location Display (CLD) System

The CLD haptic system consists of the combination of a custom designed CLD and a PHANToM force feedback device. The CLD conveys contact location information to the user's fingerpad using a linear 1-DOF actuator attached to the user's forearm and sheathed push-pull wires that connected the actuator to a roller (see Fig. 1). The user's fingertip is held by a thimble with an opening at the bottom, under which lies a roller that portrays the rendered contact location. Readings from the position encoders on the PHANToM, the angular encoder attached to the CLD gimbal and the encoder for the relative position of the roller on the fingertip are used to calculate the position and orientation of the fingertip in virtual space.
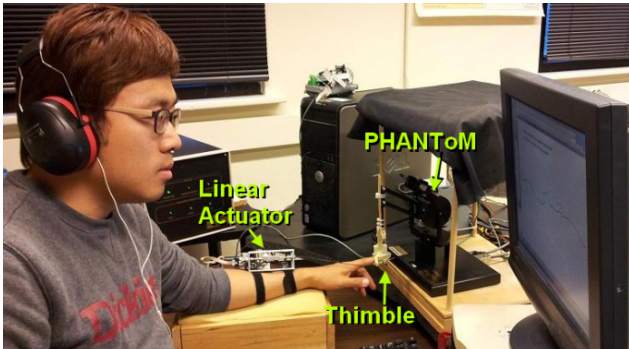

Figure 1. Experimental setup. The black curtain covers the left hand during the experiment.

The contact location is rendered by the positioning of the cylindrical roller suspended beneath the user's fingertip. The roller has a radius of 4.8 mm and the range of its motion relative to the finger is constrained to be 18 mm in software. The contact location is rendered by a relative movement of the roller on the user's fingertip using the actuated pair of push-pull wires. The nominal resolution of the roller position is 0.17 um. A PID controller is used to position the roller to a desired position. More details of the hardware and the controller are described in [15].

2.2 Stimuli

A set of thirty-one virtual stimuli are designed in the form of a slowly-varying base shape with superimposed bumps (see Fig. 2 for an example of the stimulus shape). Since the CLD used in the present study is 1-DOF, all stimuli are represented as a 2D contour shape formed from a sampled sum-of-sinusoids augmented with procedurally-generated bumps. The base shape is formed by summing twenty sinusoids with randomly-generated amplitudes (10 to 20 cm), frequencies (3 to 6 cycles/m), phases (0 to 2π) and DC offsets (–20 to 20 cm), as represented by the following equation:

$$base\_shape(x) = \sum_{i=1}^{20} (A_i \sin(2\pi f_i x + \Theta_i) + offset_i) \qquad (1)$$

After all the parameters are randomly generated, the base shape is normalized to vertically span 20 cm in height, considering the workspace of the PHANToM used for the experiment.
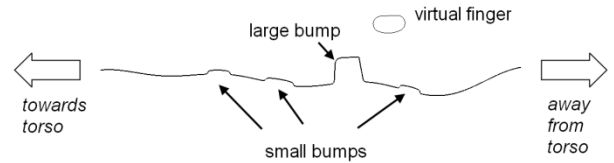

Figure 2. An example of a stimulus profile consisting of one large and three small bumps on a slowly-varying base shape, and its scale relative to the virtual finger.

The local features to be identified are defined as bumps with two different heights. The small bump has a fixed height of 3 mm and a random width of between 15 and 30 mm. The large bump has a fixed height of 18 mm and a random width of between 15 and 30 mm (Fig. 2). The bumps are then added to the base shape. The spacing between bumps is randomly chosen between the range 15 to 57 mm and averaged 28 mm. For each stimulus, a total of 0 to 4 bumps are added to a randomly-generated base contour. Of the thirty-one stimulus alternatives, 1 has no bump on the base shape, 2 have 1 bump, 4 have 2 bumps, 8 have 3 bumps, and 16 have 4 bumps.

Two rendering conditions are used in the experiment: force only (F) and force with contact location display (F+CLD). In the F condition, force information is delivered to the user through the PHANToM whenever there is a collision between the virtual finger and the virtual stimulus contour. The roller position is fixed at the center of a user's fingertip in order not to provide contact location information. In the F+CLD condition, along with the force information, contact location information is available to the user through movement of the CLD roller on the fingertip.

2.3 Haptic Rendering

The haptic rendering and control algorithms are implemented in Visual C++ using the OpenGL library and OpenHaptics toolkit (www.sensable.com). The portion of the user's fingertip that can make contact with the virtual environment is represented in 2D as a circular arc with a radius of 20 mm (Fig. 2). The position of the virtual fingertip is updated at 1 kHz, based on the readings of PHANToM position encoders and the gimbal's angle encoder.

The geometrically complex stimuli described in the previous section and the characteristics of CLD system impose several constraints on the representation of stimuli in the haptic rendering algorithm. As it is difficult to express the stimulus shapes in closed form, the contour shapes are approximated with polygonal envelopes. With this representation, however, contact location information cannot be smoothly rendered as shown by Doxon et al. [16]. Consequently, the stimuli for the present study are

represented in the form of curved contours derived from the polygonal envelopes, which is formed by sampling points on the base shape as generated by Eqn (1) at an interval of 2 mm and inserting 10 control points for the bumps. Considering that all stimuli are represented in a 2D plane and that any two adjacent curves are supposed to meet continuously in position and slope, the curved contours are represented as quadratic Bézier curves. Figure 3 shows an example of how a curved segment for two adjacent lines, AB and BC, are formed. A point P on the curved segment is represented as

$$P = (1-t)^2 A' + 2t(1-t)B + t^2 B' , \qquad (2)$$

where A′ and B′ are the midpoints of the line segments AB and BC, respectively ($0 \le t \le 1$, Fig. 3). Since the tangents of a Bézier curve at the end points are the same as those of its defining line segments, two adjacent curves always meet with the same slope. Figure 3 shows two adjacent curves (red and blue) whose slopes at point B' are the same (i.e., along the line segment $\overline{BC}$).
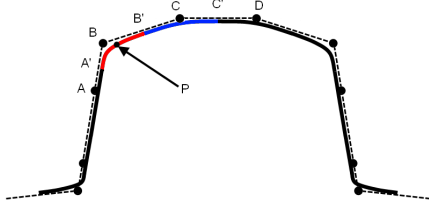

Figure 3. An example of a bump formed with 10 curve segments (solid line) to fit polygonal envelopes (dashed line) with 10 control points. The red curve is formed from line segments A'B and BB' and the blue from B'C and CC'.

Given that the experiment stimuli are made up of curve segments, the haptic rendering algorithm for the present study has to: 1) render interaction forces between curves, 2) ensure continuous forces, and 3) handle multiple contact points that occur when the virtual finger is in contact with the concave region of a stimulus (e.g., at the onset of a bump). For 1), the interaction force between two objects is calculated from the minimum distance between two contours ($F = -kx$ where x is the collision depth; $k = 1.3$ N/mm). The minimum distance is calculated as the minimum value of the distance between two freely chosen points P_A and P_B on contours A and B, which is expressed as min $|P_A - P_B|$. Piegel and Tiller derive simple equations for a point pair on two curved surfaces whose distance is the minimum [18]. For two curved contours $A(u)$ and $B(v)$, the minimum-distance points on each contour, P_A and P_B, are to satisfy the following equation with u and v as the curve parameters ($0 \le u \le 1, 0 \le v \le 1$).

$$(A(u) - B(v)) \cdot \frac{\partial A(u)}{\partial u} = 0, (A(u) - B(v)) \cdot \frac{\partial B(v)}{\partial v} = 0 \qquad (3)$$

Geometrically, this equation means that the vector between the two points $P_A - P_B$ is orthogonal to the tangent on each curve. If we define a measure d that is an inner product of $P_A - P_B$ and a unit length normal vector at P_B, when there is no collision between the two contours, d will be positive and the same as the distance between two surfaces. If there is a collision, the collision depth to render the contact force between two contours can be calculated from d and the direction of force can be calculated from the difference vector. Additionally, to satisfy requirements 2) and 3), we propose a new scheme that we termed "contact point tracing." Tracing of a contact point pair is initialized if a newly found contact point pair satisfies Eqn. (3) and d is zero or positive (See Fig. 4). Once a contact point pair is found in the current haptic servo-loop, the curve segment where the point located is

recorded. If the update rate of haptic servo-loop is high enough, the contact point should not move out of the curve segment or its nearby segments. In the next servo-loop, the recorded curve segment and its adjacent curve segments are checked to see if one of them satisfies Eqn. (3). If there is such a curve segment, the point resulting from the equation should be the updated position of the contact point in the previous servo-loop and the contact point is traced. When there are multiple contacts, the force exerted to the fingertip is calculated as the sum of the forces at each contact point pair. This way, multiple contact points can be handled and continuous force exertion is ensured because the contact force is exerted only for the contact point pair that has been traced from when d was positive. Thus, constraints 2) and 3) are satisfied by contact point tracing.
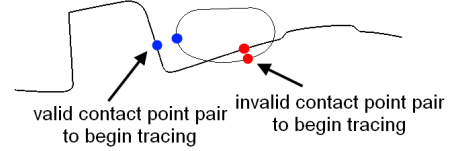

Figure 4. An example of valid and invalid contact point pair for starting contact point tracing

The mechanical structure of the CLD system imposes one more constraint on the display of contact information: only one contact point can be rendered because there is only one roller that can touch the user's fingertip. If there is only one contact point from a collision, the target position for the roller is the nearest position to the contact point on the virtual finger surface. The method is, however, not valid if there are multiple contact points from a collision. In the present study, when multiple contact points occur (typically two), the roller is placed at the point amongst the multiple contact points whose displacement is the minimum from the previous roller position (i.e., the roller will not jump to the new contact position unless it becomes a single point contact). With this approach, the movement of the roller at the fingertip is minimized, thereby allowing stable rendering of contact locations.

2.4 Absolute Identification Experiment

The experiment was designed as an absolute identification experiment where the participant identified the total number of bumps for each stimulus shape. Since each stimulus has a total of between 0 and 4 bumps, there were five stimulus types and the participants gave the corresponding responses. A 5-by-5 confusion matrix was formed for each participant and each experimental condition. Information transfer (IT) was then calculated from the confusion matrix as a measure of the correspondence between stimuli and responses. The average IT is:

$$IT = \sum_{j=1}^{K}\sum_{i=1}^{K} P(S_i, R_j) \log_2\left(\frac{P(S_i | R_j)}{P(S_i)}\right), \qquad (4)$$

or: $IT = \sum_{j=1}^{K}\sum_{i=1}^{K} P(S_i, R_j) \log_2\left(\frac{P(S_i, R_j)}{P(S_i)P(R_j)}\right) \qquad (5)$

where $P(S_i, R_j)$ is the joint probability of stimulus S_i and R_j, $P(S_i|R_j)$ is the conditional probability of S_i given R_j, $P(S_i)$ is the *a priori* probability of S_i, $P(R_j)$ is the probability of R_j. The maximum likelihood estimate of IT, denoted as IT_{est}, is computed by approximating the underlying probabilities with the frequency of occurrence by the following equation:

$$IT_{est} = \sum_{j=1}^{K}\sum_{i=1}^{K} \frac{n_{ij}}{n} \log_2\left(\frac{n_{ij} \cdot n}{n_i \cdot n_j}\right), \qquad (6)$$

where n is the total number of trials, n_i is the number of trials in which stimulus S_i is presented, n_j is the number of trials where response R_j is given by the participant, and n_{ij} is the number of trials the participant responds with R_j when presented with stimulus S_i. The quantity 2^{ITest} is used to indicate the number of bumps that can be correctly identified without any error. More details on identification experiments can be found in [19].

2.5 Participants

Ten participants (5 females, 26 to 35 years old) took part in the experiment. None of them have any known problems with their sense of touch. All are right handed by self-report. The experimental protocol is approved by the Purdue University IRB.

2.6 Procedures

The participants traced the contours of each stimulus and counted the number of virtual bumps they encountered under two experimental conditions F and F+CLD as described in Sec. 2.2. Half of the participants completed the F condition first while the other half completed the F+CLD condition first. At each trial, the number of bumps k was randomly chosen with an *a priori* probability of 0.2 (5 alternatives). For a given k, a stimulus was randomly selected among the alternatives with exactly k bumps (1 alternative for $k = 0$; 2 alternatives for $k = 1$; 4 alternatives for $k = 2$; 8 alternatives for $k = 3$; and 16 alternatives for $k = 4$). The total number of trials was initially set to be 135, which was larger than 125 trials – the minimum number of trials recommended by Miller [20]. The first ten trials were considered "warm-up" trials and were not included in data analyses. It was noticed that the OpenHaptics API would sometimes disable force output to protect the motor from overheating. The trials during which this happened were repeated at the end of the block. Therefore, the total number of trials varied depending on how many trials had to be repeated, in order to ensure that there were 125 valid trials.

The participants wore earphones and circumaural headphones (Peltor, with a noise reduction rating of 30 dB) over the earphones to block possible audio cues or noise from the haptic devices. The participant's hand and the CLD device were covered with a black cloth to block possible visual cues. Training was available at the beginning of each block. During the training, the participant could see and feel three stimulus shapes that were presented in the same way as that in the main experiment. The training was terminated when the participant was ready.

At the beginning of each trial, no haptic stimulus was available. A virtual finger was shown visually on the computer monitor to indicate the participant's current finger position. The participant was asked to move the finger to a green dot located at the starting position of the current stimulus. When the distance of the finger to the green dot was less than 2 mm, the virtual finger and the green dot disappeared and the haptic stimuli (F or F+CLD) became available. Note that the haptic stimuli could only be felt and not seen. The participant was asked to move the virtual finger from the far side of the body towards the torso *as quickly as possible* until an audible tone was heard through the earphones. The participant was instructed to *keep the finger in contact* with the virtual stimulus contour at all times to the best of his/her ability and to *count the number of bumps* that the finger encountered. The tone was played when the participant's finger passed over a position that was 18.4 cm away from the starting position, indicating the termination of the trial. The 18.4 cm distance was determined considering the workspace of the PHANToM device. At the end of each trial, the participant was prompted to enter the number of bumps felt. In short, the participant's task was to count the number of bumps as quickly as possible while maintaining contact with the stimulus contour.

Several parameters were recorded from each trial. To measure the participant's ability to identify virtual bumps, the participant's answer for the number of total bumps was recorded. To assess the participant's ability in contour following, the number of times that the virtual finger made or broke contact with the virtual stimulus contour, the duration of the trial and the duration of contour following (where the virtual finger maintained contact with the stimulus contour) were recorded.

After each block of trials, the participant took a 10-min break. It took approximately one hour for each participant to complete the two blocks of trials for the whole experiment.

2.7 Data Analysis

Each block produced data from 125 valid trials. A 5×5 stimulus-response confusion matrix was formed for each participant under each experimental condition. IT_{est} was calculated using Eqn. (6). The proportion of correct answers was also calculated.

A series of paired t-tests were run to evaluate the differences by experimental condition for the following dependent variables: IT_{est}, proportion of correct answers, the number of times that the virtual finger made or broke contact with the stimulus contour, average trial time, and average contact time.
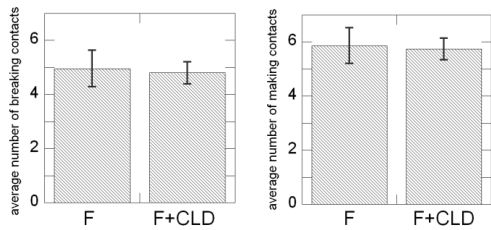
3 RESULTS

Experimental results are shown below in Fig. 5. Figure 5(a) shows the participants' average bump identification performance in terms of proportion of correct answers and information transfer. The proportion of correct answers average 64 % and 75 % for the F and F+CLD conditions, respectively. The average information transfers are 1.22 bits (2.32 items) and 1.42 bits (2.68 items) for the F and F+CLD conditions, respectively. Note that the maximum information transfer attainable for the five alternatives is 2.32 bits. In general, both bump number identification measures are higher for the F+CLD condition than for the F condition. Paired t-tests conducted for the F and F+CLD conditions indicate statistically significant differences for both the proportion of correct answers [$t(9) = 4.56$, $p < 0.01$] and for information transfer [$t(9) = 3.68$, $p < 0.01$]. Thus, we conclude that the addition of contact location information to force feedback results in improved performance of bump number identification. The results support our expectation that the availability of contact location information enhances human perception of object surface features.
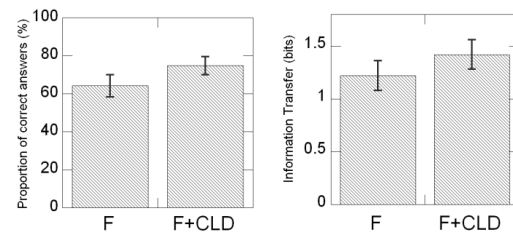
(a) Proportions of correct answers (left) and information transfer (right) for bump number identification.
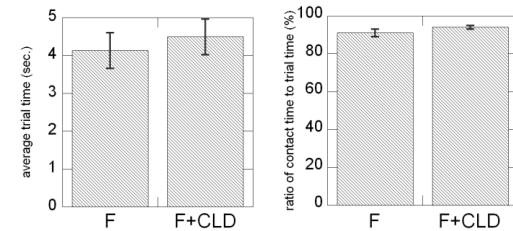
(b) Average trial time (left) and average ratio of contact time to trial time (right).

(c) Average number for breaking contact (left) between the virtual finger and a contour and average number for making contact (right) with a contour.

Figure 5. Experimental results. Error bars indicate standard errors.

Figure 5(b) shows the average recorded time for each trial and the average ratio of the amount of time the finger is in contact with the stimulus contour to the trial time. On average, it took 4.1 s and 4.5 s to complete each trial under the F and F+CLD conditions, respectively. The percentage of time the finger stayed in contact with the stimulus contour was 91% and 94% for the two conditions, respectively. There is a general trend of longer time for the F+CLD condition than that for the F condition in Fig. 5(b). However, the differences are not statistically significant for either the trial time [t(9) = 0.75, p = 0.48] or for the ratio of contact time to trial time [t(9) = 1.83, p = 0.1]. We conclude that the addition of contact location information to force feedback does not significantly affect the total exploration time, or the amount of time the finger is in contact with the stimulus contour.

Figure 5(c) shows the average number of times for breaking and making contact with the stimulus contours. On average, the participant's finger broke contact 4.9 times and 4.8 times under the F and F+CLD conditions, respectively. Participants made contact 5.9 times and 5.7 times under the two conditions. As expected, the two plots in Figure 5(c) are similar as the participants had to make a new contact every time the finger broke contact with the contour. Paired t-tests indicate no statistically significant difference between the F and F+CLD conditions for breaking contact [t(9) = 0.23, p = 0.83] or for making contact [t(9) = 0.25, p = 0.81].

Therefore, we conclude that the addition of contact location information to force feedback does not lead to an improvement in contour following as measured by the average number of times of breaking and making contact with the stimulus contours, average trial time, or average contact time. This is contrary to the earlier results suggesting that better contour following is facilitated by contact location information [11]. We explore the implications of our findings in the next section.

The results of the present study do indicate improved surface feature identification. We had hypothesized that the availability of contact location information would especially facilitate the detection of smaller surface features. To investigate this further, the proportions of correct answers for total number of bumps are computed separately for stimulus contours with small bumps only (total 4 stimuli) or with large bumps only (total 4 stimuli) (see Fig. 6). For small bumps only, the accuracies are 59% and 76% for the F and F+CLD conditions, respectively. For large bumps only, the accuracies are 87% and 91% for the two conditions. As expected, it appears that it is more difficult to count the number of small bumps accurately than to count the number of large bumps. When paired t-tests between F and F+CLD conditions are conducted, a significant difference is found for small bumps [t(9) = 2.52, p = 0.03], but not for large bumps [t(9) = 0.89, p = 0.8]. The results indicate that the participants identified the number of small bumps better when contact location information is available than when

there is only force feedback. In contrast, the availability of contact location cue does not affect the detection of large bumps.
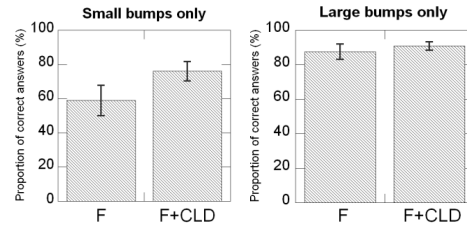

Figure 6. Average proportions of correct answers for bump number identification with small bumps only (left) and large bumps only (right). Error bars indicate standard errors.

Further analysis is conducted by grouping the stimuli by the number of small bumps they contain. The average accuracy for the F condition was subtracted from that for the F+CLD condition, to obtain a measure for the additional bumps recovered due to contact location information (see Fig. 7). As expected, since the participants' haptic perception is better for small bumps with the addition of CLD, the difference in accuracy increases as the number of small bump increases.
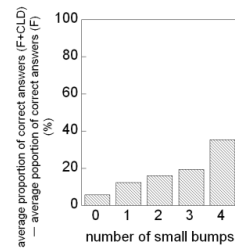

Figure 7. The difference in average proportion of correct answers for the F+CLD and F conditions.

In an additional analysis, the absolute error in the participants' responses is averaged by the number of small bumps, as follows:

$$average\_error(k)$$
$$= \sum_{i=1}^{n_k} \frac{\left| number\_of\_bumps(i) - participant's\_answer(i) \right|}{n_k} \quad (7)$$

where n_k is the total number of bump patterns with k small bumps. As seen in Fig. 8 (left panel), the absolute error increases monotonically with the number of small bumps. It therefore appears that contact location information facilitated the participants' haptic perception of bumps through improved identification of small bumps. When expressed in percentage change of error rate, the error when counting small-bumps was reduced by roughly 40% regardless of the number of small bumps (Fig. 8, right panel).
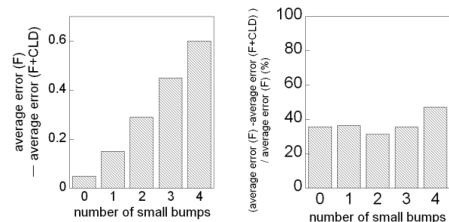

Figure 8. The difference in average error for the F and F+CLD conditions in (left) absolute and (right) relative terms.

4 Discussion and Conclusions

The present study investigated the role of contact location information in contour following and feature detection. We were particularly interested in discovering any improvement in object surface feature detection due to better contour following. The results from the experiment show larger information transfer and percent correct scores for identifying the number of virtual bumps for the F+CLD condition than for the F condition, indicating improved perception of virtual objects with the addition of contact location information. However, no significant improvement in contour following is found, as measured by contact time and number of breaks in contact, with the addition of CLD.

Our finding of no significant improvement of contour following with the addition of contact location information to force feedback is contrary to that of an earlier study by Kuchenbecker et al. [11]. This can probably be explained by the differences in methods and virtual environments between Kuchenbecker et al.'s study and the present study. In the present study, all the bumps protruded up from the contour, whereas the stimuli in [11] contained edges of a surface. It was therefore easier for the contact point to fall off the contour in [11] than in the present study. Also, it is noteworthy that in [11], there was only one downward edge and if a participant broke contact with the top or side surfaces of the contour then it was considered a failure for that trial. This might have led each participant to closely concentrate on keeping his/her finger on the surface and thus to move his/her finger more slowly than in our present study. In the present study (with a stimulus length of 18.4 cm), the average times per trial were 4.1 s and 4.5 s for the F and F+CLD conditions, respectively. In [11], the trial completion times were 10.4 s and 4.9 s for the stimuli with a width of 10 cm for the F and F+CLD conditions, respectively. It thus appears that the participants in [11] moved their fingers slower and utilized the available cues for contour following, where the addition of the contact location information made a significant difference.

Second, our result that there was no significant difference of contour following between the two experimental conditions can be explained from the contact time of the participants. As shown in Fig. 5(b), the average ratio of the contact time to the trial time across all the participants are 91 % and 94 % for the F and F+CLD conditions, respectively. In addition, the difference of the average trial time and the average contact time is small (0.3 s) for both experiment conditions. The results indicate that the participants successfully followed the instruction to "*keep the finger in contact*" (see Sec. 2.6) and were successful in contour following in both experimental conditions. Thus, we can conclude that the participants of the present study were successful in the contour following task for both the F and F+CLD conditions and the difference in the perception of local features can be attributed to the improved perception of small surface features with the addition of contact location information.

Future work will investigate the mechanism by which contact location information enhances the detection of small surface features. The following parameters will be recorded continuously: collision of virtual finger with surface contours, contact forces, and rendered contact locations on the fingertip. The data will be analyzed for both small and large bumps to gain insight on the roles force and contact location information play in surface feature detection, especially for small features. Bumps of sizes between the small and large bumps generated for the present study will be used to ascertain at what scale a feature becomes more salient with the addition of contact location information.

References

[1] A. Frisoli, M. Bergamasco, S. L. Wu, and E. Ruffaldi, "Evaluation of multipoint contact interfaces in haptic perception of shapes," *Multipoint Interaction with Real and Virtual Objects*, Springer Tracts in Advanced Robotics, 18, 177-188, 2005.

[2] G. Jansson and L. Monaci, "Identification of real objects under conditions similar to those in haptic displays: providing spatially distributed information at the contact areas is more important than increasing the number of areas," *Virtual Reality*, 9(4), 243-249, 2006.

[3] A. Frisoli, M. Solazzi, F. Salsedo, and M. Bergamasco, "A fingertip haptic display for improving curvature discrimination," *Presence: Teleoperators & Virtual Environments*, 17(6), 550-561, 2008.

[4] E. P. Scilingo, M. Bianchi, G. Grioli, and A. Bicchi, "Rendering softness: Integration of kinesthetic and cutaneous information in a haptic device," *IEEE Transactions on Haptics*, 3(2), 109-118, 2010.

[5] B. T. Gleeson, S. K. Horschel, and W. R. Provancher, "Design of a fingertip-mounted tactile display with tangential skin displacement Feedback," *IEEE Transactions on Haptics*, 3(4), 297-301, 2010.

[6] J. Luk, J. Pasquero, S. Little, K. MacLean, V. Levesque, and V. Hayward, "A role for haptics in mobile interaction: Initial design using a handheld tactile display prototype," P*roceedings of CHI'06*, 10 pp., 2006.

[7] L. Winfield, J. Glassmire, J. E. Colgate, and M. Peshkin, "T-PaD: Tactile pattern display through variable friction reduction," *Proceedings of the World Haptics Conference'07*, 421-426, 2007.

[8] I. Sarakoglou, N. Garcia-Hernandez, N. G. Tsagarakis, and D. G. Caldwell, "A High Performance Tactile Feedback Display and Its Integration in Teleoperation," *IEEE Transactions on Haptics*, 5(3), 252-263, 2012.

[9] W. R. Provancher, K. J. Kuchenbecker, G. Niemeyer, and M. R. Cutkosky, "Perception of curvature and object motion via contact location feedback," *Proceedings of the International Symposium on Robotics Research,*, 456-465, 2003.

[10] S. J. Lederman and R. L. Klatzky, "Hand movements: A window into haptic object recognition," *Cognitive Psychology*, 19(3), 342-368, 1987.

[11] K. J. Kuchenbecker, W. R. Provancher, G. Niemeyer, and M. R. Cutkosky, "Haptic display of contact location," *Proceedings of the IEEE Haptics Symposium*, 40-47, 2004.

[12] S. Hsiao, "Central mechanisms of tactile shape perception," *Current Opinion in Neurobiology*, 18(4), 418-424, 2008.

[13] M. A. Srinivasan and R. H. LaMotte, "Encoding of shape in the responses of cutaneous mechanoreceptors," *Information Processing in the Somatosensory Systems*, O. Franzen and J. Westman, Eds.: MacMillan Press, 59-69, 1991.

[14] A. B. Vallbo and R. S. Johansson, "Properties of cutaneous mechanoreceptors in the human hand related to touch sensation," *Human Neurobiology*, 3(1), 3-14, 1984.

[15] W. R. Provancher, M. R. Cutkosky, K. J. Kuchenbecker, and G. Niemeyer, "Contact location displays for haptic perception of curvature and object motion," *The International Journal of Robotics Research*, 24(9), 691-702, 2005.

[16] A. J. Doxon, D. E. Johnson, H. Z. Tan, and W. R. Provancher, "Force and Contact Location Shading Thresholds for Smoothly Rendering Polygonal Models," *Proceedings of the Haptics Symposium,* 183-190, 2010.

[17] J. Park, A. J. Doxon, W. R. Provancher, D. E. Johnson, and H. Z. Tan, "Edge sharpness perception with force and contact location information," *Proceedings of the World Haptics Conference*, 517-522, 2011.

[18] L. Piegel and W. Tiller, *The NURBS book*. Berlin: Springer-Verlag, 1995.

[19] H.-Y. Chen, J. Park, S. Dai, and H. Z. Tan, "Design and evaluation of identifiable key-click signals for mobile devices," *IEEE Transactions on Haptics*, 4(4), 229-241, 2011.

[20] G. A. Miller, "Note on the bias of information estimates," in *Information Theory in Psychophysics*, 95-100, 1954.